J Mater Sci (2007) 42:1901–1908
DOI 10.1007/s10853-006-0345-8

NONSTOICHIOMETRIC COMPOUNDS

Oxygen nonstoichiometry and defect structure of undoped and doped lanthanum cobaltites

A. Yu. Zuev · A. N. Petrov · A. I. Vylkov ·
D. S. Tsvetkov

Received: 30 November 2005 / Accepted: 17 April 2006 / Published online: 18 January 2007

Abstract The results of oxygen nonstoichiometry are presented for the perovskite-type undoped cobaltite $LaCoO_{3-\delta}$, doped with strontium $La_{0.7}Sr_{0.3}CoO_{3-\delta}$, and doped with copper $LaCo_{0.7}Cu_{0.3}O_{3-\delta}$ as a function of oxygen partial pressure p_{O_2} and temperature. The modeling of the defect structure of these oxygen deficient perovskites is carried out. Two different defect structure models are evolved. Within the framework of the first model electrons are treated as quasi-free in $LaCoO_{3-\delta}$, partly trapped in $La_{0.7}Sr_{0.3}CoO_{3-\delta}$ and $LaCo_{0.7}Cu_{0.3}O_{3-\delta}$, whereas holes are assumed to be itinerant in all oxides studied. The intrinsic electronic disordering process is taken into account as well. According to the second model electrons and holes are assumed to be localized. Thermal excited charge disproportionation of cobalt is considered as well. The corresponding equations for the law of mass action, electroneutrality condition, and mass balance give a set of nonlinear equations in the both cases. The analytical solutions of these sets yield general expressions which are used for the verification of the defect models proposed by nonlinear curve fitting. The latter showed that both models of the defect structure of all lanthanum cobaltites studied fit the experimental data about equally good. It is, therefore, difficult to rule out either of defect structure models on the basis of equilibrium data on oxygen nonstoichiometry solely.

Introduction

The perovskite-type doped lanthanum cobaltites have already attracted great attention as cathode materials for high temperature solid oxide fuel cells (SOFC) due to their high melting point, large electronic conductivity, relatively large oxygen ionic conductivity, and high chemical stability in oxidizing environments at high temperature (700–1000 °C). They are also known as the-state-of-the-art materials for oxidation catalysts, gas separation membranes, CO2 laser cathodes, and sensors. The properties required for such application are generally adjusted by doping $LaCoO_3$ with heterovalent cations on La and Co sites. The substitution of Sr for lanthanum increases both the electronic and oxide ion conductivity of lanthanum cobaltite by introducing of hole carriers and oxygen vacancies, respectively [1]. The substitution of transition metal such as Cu for cobalt has been found to lead to increase of oxygen nonstoichiometry and improve substantially the electrocatalytic activity of the cathodes on the basis of $LaCoO_3$ [2, 3]. It is known that important properties of doped lanthanum cobaltites such as oxide ion and electrical conductivity in ambient atmosphere are directly related to their defect structure. Sr-doped lanthanum cobaltite received most attention in this respect. The oxygen nonstoichiometry and defect structure of $La_{1-x}Sr_xCoO_{3-\delta}$ were studied by Mizusaki et al. [4], Petrov et al. [5, 6], Lankhorst et al. [7–9], and Kozhevnikov et al. [10, 11]. Lankhorst et al. [7–9] described the defect structure of $La_{1-x}Sr_xCoO_{3-\delta}$ ($x = 0.2, 0.4, 0.7$) in the framework of the electron gas rigid band model by assumption that electrons created during vacancy formation are placed in broad electron band [8]. Contrary to the conclusions of

A. Yu.Zuev (✉) · A. N. Petrov · A. I. Vylkov ·
D. S. Tsvetkov
Chemical Department, Ural State University, Lenin Av.51,
Yekaterinburg 620083, Russia
e-mail: andrew.zuev@usu.ru

Lankhorst et al. [7–9] $La_{1-x}Sr_xCoO_{3-\delta}$ ($x = 0.3, 0.6$) was shown by Kozhevnikov et al. [10, 11] to be a typical narrow band conductor at elevated temperatures. Mizusaki et al. [4] emphasized that $La_{1-x}Sr_xCoO_{3-\delta}$ is not a wide-band gap semiconductor since there is no plateau on p_{O_2} dependences of its oxygen nonstoichiometry at $\delta = x/2$. The electrons were, therefore, concluded to be not strongly localized on Co ions.

The oxygen nonstoichiometry of Cu-doped lanthanum cobaltite was measured and some preliminary results on its defect structure were reported by us earlier [2, 12, 13].

The oxygen nonstoichiometry of undoped $LaCoO_3$ was studied only in few works to date. First Seppaenen et al. [14] measured it as a function of p_{O_2} by use of coulometric titration technique in temperature range between 900 and 1038 °C. Randomly distributed oxygen vacancies with different charges were assumed to be anionic defects in $LaCoO_3$. Later Petrov et al. [15] studied oxygen nonstoichiometry of $LaCoO_{3-\delta}$ as a function of p_{O_2} using TGA method in high temperature range $1000 \le T, ^\circ C \le 1300$. The oxygen nonstoichiometry of $LaCoO_{3-\delta}$ was also studied by Mizusaki et al. [4] on single crystal sample at moderate temperatures between 900 and 1000 °C. The defect structure of this oxide was discussed by them in terms of partial molar enthalpy and entropy of oxygen. It is necessary to note that values of oxygen nonstoichiometry of $LaCoO_{3-\delta}$ reported by Mizusaki et al. [4] exceed those measured by Seppaenen et al. [14] by about an order of magnitude at low p_{O_2} and the same temperature. There are no data concerning the quantitative modeling of the defect structure of undoped lanthanum cobaltite to date.

All mentioned above gives rise to draw a conclusion that despite intense interest over the past decades, the defect structure of undoped and doped lanthanum cobaltites remains a controversial topic of discussion. The elucidation of this defect structure by the quantitative modeling on the basis of precise measurement of oxygen nonstoichiometry is, therefore, the priority aim of the present study.

Experimental

Powder of selected undoped, Sr- and Cu-doped lanthanum cobaltites was synthesized by solid state chemical reaction from the corresponding component oxides and carbonates according to technique described elsewhere [2, 5, 15] The phase composition and the crystal structure of a sample was determined by means of X-ray diffraction, XRD, with a Dron-6 diffractometer using Cu K_α radiation. XRD showed no indication for the presence of a second phase. The single phase powders were used further for oxygen nonstoichiometry measurement. Changes in oxygen stoichiometry of Cu-doped lanthanum cobaltite were investigated using TGA technique as a function of the oxygen partial pressure and temperature. The experimental setup developed by us for the thermogravimetric measurement at different oxygen partial pressures is described elsewhere [2]. Oxygen nonstoichiometry of undoped and Sr-doped [11] lanthanum cobaltites was measured as a function of the oxygen partial pressure and temperature by use of coulometric titration technique described elsewhere [2, 11]. After the oxygen nonstoichiometry measurements the samples of doped cobaltites investigated were reduced in pure hydrogen gas at temperature of 900 °C directly into the thermogravimetric device in order to determine the absolute values of the oxygen nonstoichiometry. The sample of undoped $LaCoO_{3-\delta}$ was reduced at 900 °C in the same way. After reduction by H_2 gas, XRD analysis was performed as fast as possible to confirm that the samples had been reduced to the mixture of appropriate oxides (La_2O_3, SrO) and metals (Cu, Co).

Theory

Models of the defect structure of undoped and Sr-doped $LaCoO_{3-\delta}$

Since the oxygen nonstoichiometry seems to have relatively low values, let us consider only randomly distributed point defects. Let us assume also that Sr as a dopant on A site traps electron and can be, therefore, written as Sr'_{La} using the Kröger–Vink notation. Strontium is believed to keep its oxidation state of 2+ as a constant irrespective of p_{O_2} and temperature. The concentration of Sr'_{La} may be, therefore, simply replaced by total concentration of the dopant x. Moreover, it is not clear so far whether electrons which are not trapped on Sr sites and holes are delocalized or localized on cobalt sites in cobaltite lattice. Two different models should be, therefore, considered here and hereafter.

If within the framework of *model 1* the approach of itinerant electronic species is accepted, then the condition of charge neutrality is given as:

$$p + 2[V_O^{\cdot\cdot}] = n + x \tag{1}$$

Let us accept the approach of electrons and holes localized on Co sites in the *model 2* of the defect structure of $\mathrm{La}_{1\text{-}x}\mathrm{Sr}_x\mathrm{CoO}_{3\text{-}\delta}$. In that case the condition of charge neutrality is written as:

$$[\mathrm{Co}^{\cdot}_{\mathrm{Co}}] + 2[\mathrm{V}^{\cdot\cdot}_{\mathrm{O}}] = [\mathrm{Co}'_{\mathrm{Co}}] + x, \tag{1a}$$

where $\mathrm{Co}'_{\mathrm{Co}}$ and $\mathrm{Co}^{\cdot}_{\mathrm{Co}}$ are electron and hole, respectively, localized on Co site and expressed using the Kröger–Vink notation. Intrinsic disordering

$$\mathrm{nil} = e' + h^{\cdot} \tag{2}$$

with equilibrium constant

$$K_2 = np \tag{3}$$

should be taken into account for $\mathrm{La}_{1\text{-}x}\mathrm{Sr}_x\mathrm{CoO}_{3\text{-}\delta}$ within the framework of the *model 1*. The reaction of charge disproportionation involving the transfer of an electron between adjacent $\mathrm{Co}^{\times}_{\mathrm{Co}}$ sites

$$2\mathrm{Co}^{\times}_{\mathrm{Co}} = \mathrm{Co}'_{\mathrm{Co}} + \mathrm{Co}^{\cdot}_{\mathrm{Co}} \tag{4}$$

with equilibrium constant

$$K_4 = \frac{[\mathrm{Co}'_{\mathrm{Co}}][\mathrm{Co}^{\cdot}_{\mathrm{Co}}]}{[\mathrm{Co}^{\times}_{\mathrm{Co}}]^2} \tag{5}$$

should be considered in *model 2* accordingly. Furthermore, the process of oxygen release from the cobaltite lattice under reducing conditions is accompanied by the holes consumption (*model 1*)

$$\mathrm{O}^{\times}_{\mathrm{O}} + 2h^{\cdot} = \frac{1}{2}\mathrm{O}_2 + \mathrm{V}^{\cdot\cdot}_{\mathrm{O}} \tag{6}$$

or by reduction of Co^{4+} to Co^{3+} according to the following reaction (*model 2*)

$$\mathrm{O}^{\times}_{\mathrm{O}} + 2\mathrm{Co}^{\cdot}_{\mathrm{Co}} = \frac{1}{2}\mathrm{O}_2 + \mathrm{V}^{\cdot\cdot}_{\mathrm{O}} + 2\mathrm{Co}^{\times}_{\mathrm{Co}} \tag{7}$$

The equilibrium constants of the reactions Eqs. 6 and 7 can be given as

$$K_6 = \frac{[\mathrm{V}^{\cdot\cdot}_{\mathrm{O}}]p^{0.5}_{\mathrm{O}_2}}{[\mathrm{O}^{\times}_{\mathrm{O}}]p^2} \tag{8}$$

$$K_7 = \frac{[\mathrm{V}^{\cdot\cdot}_{\mathrm{O}}][\mathrm{Co}^{\times}_{\mathrm{Co}}]^2 p^{0.5}_{\mathrm{O}_2}}{[\mathrm{O}^{\times}_{\mathrm{O}}][\mathrm{Co}^{\cdot}_{\mathrm{Co}}]^2} \tag{9}$$

Combination of aforementioned reactions allows to derive other defects reactions. Subtraction of Eq. 4 from Eq. 7, for instance, yields the following reaction of the defect formation

$$\mathrm{O}^{\times}_{\mathrm{O}} + 2\mathrm{Co}^{\times}_{\mathrm{Co}} = \frac{1}{2}\mathrm{O}_2 + \mathrm{V}^{\cdot\cdot}_{\mathrm{O}} + 2\mathrm{Co}'_{\mathrm{Co}} \tag{10}$$

with equilibrium constant

$$K_{10} = \frac{[\mathrm{V}^{\cdot\cdot}_{\mathrm{O}}][\mathrm{Co}'_{\mathrm{Co}}]^2 p^{0.5}_{\mathrm{O}_2}}{[\mathrm{O}^{\times}_{\mathrm{O}}][\mathrm{Co}^{\times}_{\mathrm{Co}}]^2} \tag{11}$$

It is evident that only two reactions from Eqs. 4, 7, and 10 are independent from each other and, therefore, may be used for modeling.

By taking into account the balance mass condition and obvious definitions $[\mathrm{V}^{\cdot\cdot}_{\mathrm{O}}] = \delta$ the following sets of nonlinear equation can be given for the models described above:

Model 1.

$$\begin{cases} K_2 = np = K^o_2 \exp\left(-\frac{\Delta H^o_2}{RT}\right) \\ K_6 = \frac{\delta p^{0.5}_{\mathrm{O}_2}}{(3-\delta)p^2} = K^o_6 \exp\left(-\frac{\Delta H^o_6}{RT}\right) \\ p + 2\delta = n + x \end{cases}. \tag{12}$$

The analytical solutions of this set with physical meaning are the concentration of holes

$$p = \frac{x}{2} + \frac{\sqrt{4\delta^2 - 4\delta x + x^2 + 4K_2}}{2} - \delta = f_h(T,\delta) \text{ and} \tag{13}$$

$$\log(p_{\mathrm{O}_2}/atm) = 4\log\left(\frac{\sqrt{K_6}\sqrt{3-\delta}\left(2\delta - x - \sqrt{4\delta^2 - 4\delta x + x^2 + 4K_2}\right)}{-2\sqrt{\delta}}\right) \tag{14}$$

Model 2.

$$\begin{cases} K_4 = \frac{[Co'_{Co}][Co^{\cdot}_{Co}]}{[Co^{\times}_{Co}]^2} = K^o_4 \exp\left(-\frac{\Delta H^o_4}{RT}\right) \\ K_{10} = \frac{\delta[\mathrm{Co}'_{\mathrm{Co}}]^2 p^{0.5}_{\mathrm{O}_2}}{(3-\delta)[\mathrm{Co}^{\times}_{\mathrm{Co}}]^2} = K^o_{10} \exp\left(-\frac{\Delta H^o_{10}}{RT}\right) \\ [\mathrm{Co}^{\cdot}_{\mathrm{Co}}] + 2\delta = [\mathrm{Co}'_{\mathrm{Co}}] + x \\ [\mathrm{Co}^{\cdot}_{\mathrm{Co}}] + [\mathrm{Co}'_{\mathrm{Co}}] + [\mathrm{Co}^{\times}_{\mathrm{Co}}] = 1 \end{cases}. \tag{15}$$

The analytical solutions of this set with physical meaning are the concentration of localized electrons

$$[\mathrm{Co}'_{\mathrm{Co}}] = \frac{4K_4 - 4K_4x + x + 8K_4\delta - 2\delta + C}{2(4K_4 - 1)} = f_{\mathrm{Co}'_{\mathrm{Co}}}(T,\delta) \tag{16}$$

and

$$\log(p_{\mathrm{O}_2}/atm) = 4\log\left\{\frac{2\sqrt{K_{10}}\sqrt{(3-\delta)}(-1-C)}{(4K_4-4K_4x+x+8K_4\delta-2\delta+C)\cdot\sqrt{\delta}}\right\}, \tag{17}$$

where $C=-\sqrt{4K_4+4\delta^2-4x\delta+x^2-4K_4x^2-16K_4\delta^2+16K_4\delta^2}$.

The equations Eq. 14 and Eq. 17 can be used further for the fitting of defect *model 1* and *model 2*, respectively, by experimental data on the oxygen nonstoichiometry of $\mathrm{La}_{1\text{-}x}\mathrm{Sr}_x\mathrm{CoO}_{3\text{-}\delta}$. All symbol manipulations in this work were carried out by the use of the advanced mathematics software Maple 9.5 (Waterloo Maple Inc., Waterloo, Canada).

Models of the defect structure of Cu-doped lanthanum cobaltite

It was found by us earlier [2, 12, 13] that partial replacement of cobalt by copper caused a substantial increase of oxygen deficiency in the $\mathrm{LaCo}_{1\text{-}x}\mathrm{Cu}_x\mathrm{O}_{3\text{-}\delta}$ oxides. This is evident that copper introduced into the cobalt sublattice becomes an electron acceptor ($\mathrm{Cu}'_{\mathrm{Co}}$), since copper is more electronegative as compared to cobalt. The negative charge excess of acceptor defects in the oxide structure is balanced by the corresponding amount of positive charges, which can be oxygen vacancies and/or electron holes. The formation of equilibrium electronic point defects can be described again within the framework of either quasi-free ($h^{\cdot}$) or localized holes ($\mathrm{Co}^{\cdot}_{\mathrm{Co}}$) models. Then the charge neutrality condition in the case of itinerant nature of electrons and holes in the Co-doped lanthanum cobaltite (*model 1A*) is given as

$$p+2[V^{\cdot\cdot}_O]=n+[\mathrm{Cu}'_{\mathrm{Co}}] \tag{18}$$

Within the framework of localized nature of electronic species in $\mathrm{LaCo}_{1\text{-}x}\mathrm{Cu}_x\mathrm{O}_{3\text{-}\delta}$ (*model 2A*) the charge neutrality condition requires that

$$[\mathrm{Co}^{\cdot}_{\mathrm{Co}}]+2[\mathrm{V}^{\cdot\cdot}_{\mathrm{O}}]=[\mathrm{Cu}'_{\mathrm{Co}}]+[\mathrm{Co}'_{\mathrm{Co}}] \tag{19}$$

Copper can change its oxidation state depending on p_{O_2} and temperature unlike strontium. The concentration of $\mathrm{Cu}'_{\mathrm{Co}}$ cannot be, therefore, simply replaced by total concentration of the dopant x in Eq. 18 and Eq. 19 and the following reactions

$$\mathrm{Cu}^{\times}_{\mathrm{Cu}}=\mathrm{Cu}'_{\mathrm{Cu}}+h^{\cdot} \tag{20}$$

with the equilibrium constant

$$K_{20}=\frac{[\mathrm{Cu}'_{\mathrm{Co}}]p}{[\mathrm{Cu}^{\times}_{\mathrm{Co}}]}\text{ and} \tag{21}$$

$$\mathrm{Cu}^{\times}_{\mathrm{Co}}+\mathrm{Co}^{\times}_{\mathrm{Co}}=\mathrm{Cu}'_{\mathrm{Co}}+\mathrm{Co}^{\cdot}_{\mathrm{Co}} \tag{22}$$

with the equilibrium constant

$$K_{22}=\frac{[\mathrm{Cu}'_{\mathrm{Co}}][\mathrm{Co}^{\cdot}_{\mathrm{Co}}]}{[\mathrm{Cu}^{\times}_{\mathrm{Co}}][\mathrm{Co}^{\times}_{\mathrm{Co}}]} \tag{23}$$

should be taken into account in *model 1A* and *model 2A*, respectively. Assuming further that defects reactions Eqs. 2 and 6 or Eqs. 4 and 7 are valid for $\mathrm{LaCo}_{1\text{-}x}\mathrm{Cu}_x\mathrm{O}_{3\text{-}\delta}$ depending on a model. Then addition of reactions Eq. 6 and Eq. 20 or Eq. 7 and Eq. 22 gives us reaction describing uptake or release of oxygen by oxide with participation of copper in cobalt sublattice

$$\mathrm{O}^{\times}_{\mathrm{O}}+2\mathrm{Cu}^{\times}_{\mathrm{Co}}=\frac{1}{2}\mathrm{O}_2+\mathrm{V}^{\cdot\cdot}_{\mathrm{O}}+2\mathrm{Cu}'_{\mathrm{Co}} \tag{24}$$

the equilibrium constants of which is given as

$$K_{24}=\frac{[\mathrm{V}^{\cdot\cdot}_{\mathrm{O}}][\mathrm{Cu}'_{\mathrm{Co}}]^2p^{0.5}_{\mathrm{O}_2}}{[\mathrm{O}^{\times}_{\mathrm{O}}][\mathrm{Cu}^{\times}_{\mathrm{Co}}]^2}. \tag{25}$$

Reactions Eqs. 2, 20, and 24 or Eqs. 4, 22, and 24 are independent from each other and, therefore, may be used for modeling. By taking into account the balance mass condition and obvious definitions $[\mathrm{V}^{\cdot\cdot}_{\mathrm{O}}]=\delta$ the following sets of nonlinear equation can be given for the models described above:

Model 1A.

$$\left\{\begin{array}{c} K_2=np=K^o_2\exp\left(-\frac{\Delta H^o_2}{RT}\right)\\ K_{20}=\frac{[\mathrm{Cu}'_{\mathrm{Co}}]p}{[\mathrm{Cu}^{\times}_{\mathrm{Co}}]}=K^{\mathrm{o}}_{20}\exp\left(-\frac{\Delta H^{\mathrm{o}}_{20}}{RT}\right)\\ K_{24}=\frac{[\mathrm{V}^{\cdot\cdot}_{\mathrm{O}}][\mathrm{Cu}'_{\mathrm{Co}}]^2p^{0.5}_{\mathrm{O}_2}}{[\mathrm{O}^{\times}_{\mathrm{O}}][\mathrm{Cu}^{\times}_{\mathrm{Co}}]^2}=K^o_{24}\exp\left(-\frac{\Delta H^{\mathrm{o}}_{24}}{RT}\right)\\ p+2\delta=n+[\mathrm{Cu}'_{\mathrm{Co}}]\\ [\mathrm{Cu}'_{\mathrm{Co}}]+[\mathrm{Cu}^{\times}_{\mathrm{Co}}]=x \end{array}\right. \tag{26}$$

These combined equations can be solved analytically to obtain necessary model equation. By successive substitution the following cubic equation with respect to concentration of quasi-free holes can be derived

$$ap^3+bp^2+cp-d=0. \tag{27}$$

The analytical solutions of this equation with physical meaning is the concentration of itinerant holes

$$p = \frac{B^{1/3}}{6} - \frac{6\left(\frac{c}{3} - \frac{b^2}{9}\right)}{B^{1/3}} - \frac{b}{3} = f_h(T, \delta), \tag{28}$$

where $a = 1, b = (2\delta + K_{20}), c = (-K_{20}\,x + 2\delta K_{20} - K_2)$, $d = K_2\,K_{20}$ and

$$B = 36cb - 108d - 8b^3 + 12\sqrt{12c^3 - 3c^2b^2 - 54cbd + 81d^2 + 12db^3}$$

Substitution of Eq. 28 in Eq. 25 using the charge neutrality and mass balance conditions yields a necessary model equation

$$\log(p_{\mathrm{O}_2}/atm) = 4\log\left(\frac{K_{24}^{0.5}(3-\delta)^{0.5}\left(x - \frac{K_{20}x}{D}\right)D}{K_{20}x\delta^{0.5}}\right), \tag{29}$$

where $D = K_{20} + \frac{B}{6} - \frac{2(3c-b^2)}{3B} - \frac{b}{3}$.

Model 2A.

The set of nonlinear equations now consists of expressions for equilibrium constant Eqs. 5, 23, 25 and charge neutrality condition Eq. 19 along with mass balance conditions $[\mathrm{Cu}^{\times}_{\mathrm{Co}}] + [\mathrm{Cu}'_{\mathrm{Co}}] = x$, and $[\mathrm{Co}^{\times}_{\mathrm{Co}}] + [\mathrm{Co}^{\cdot}_{\mathrm{Co}}] + [\mathrm{Co}^{\cdot}_{\mathrm{Co}}] = 1 - x$. Appropriate substitutions lead to the cubic equation with respect to concentration of divalent copper $\mathrm{Cu}'_{\mathrm{Co}}$

$$a[\mathrm{Cu}'_{\mathrm{Co}}]^3 + b[\mathrm{Cu}'_{\mathrm{Co}}]^2 + c[\mathrm{Cu}'_{\mathrm{Co}}] + d = 0, \tag{30}$$

where $a = K_4 + K_{22}^2 - K_{22}$, $b = K_4(1 - x - 2\delta) + K_{22}(x - K_4x - K_4 - 2K_4\delta + 2\delta)$, and $c = K_4(2K_4x - K_4x^2 + 4K_4\delta x - 2\delta x)$, $d = K_4(-K_4x^2 + K_4x^3 - 2K_4\delta x^2)$. The solution of the cubic equation with a physical meaning allowed to express p_{O_2} explicitly from Eq. 25 as a function of oxygen nonstoichiometry to verify whether the *model* 2*A* fits the experimental data. This expression is similar to that discussed for the previous model and, therefore, it is omitted here.

Results and discussion

All cobaltite compositions $\mathrm{La}_{1\text{-}x}\mathrm{Sr}_x\mathrm{CoO}_{3\text{-}\delta}$ (x = 0, 0.3) and $\mathrm{LaCo}_{0.7}\mathrm{Cu}_{0.3}\mathrm{O}_{3\text{-}\delta}$ have a hexagonal structure according to XRD analysis. The structural parameters of these compounds were refined based on *R*–3*c* space group using Rietveld analysis and are given in Table 1.

Table 1 Structure parameters for $\mathrm{La}_{1\text{-}x}\mathrm{Sr}_x\mathrm{CoO}_{3\text{-}\delta}$ (x = 0, 0.3) and $\mathrm{LaCo}_{0.7}\mathrm{Cu}_{0.3}\mathrm{O}_{3\text{-}\delta}$

LaCoO_3	a = 5.4440(3) Å,	c = 13.092(1)Å,	V = 335.85(5)Å,
$\mathrm{La}_{0.7}\mathrm{Sr}_{0.3}\mathrm{CoO}_3$	a = 5.4406(3)Å,	c = 13.1950(8)Å,	V = 338.25(4)Å
$\mathrm{LaCo}_{0.7}\mathrm{Cu}_{0.3}\mathrm{O}_3$	a = 5.472(3)Å,	c = 13.135(1)Å,	V = 340.57(5)Å

Absolute value of oxygen nonstoichiometry in $\mathrm{LaCoO}_{3\text{-}\delta}$ determined by reduction in hydrogen amounted to 0.003 ± 0.002 at 1000 °C in air. Value of the oxygen nonstoichiometry obtained in that way for $\mathrm{LaCoO}_{3\text{-}\delta}$ cannot be regarded as satisfactory unlike other lanthanum cobaltite compositions studied in this work. It is worth to note that the experimental determination of an absolute value of oxygen nonstoichiometry is a known problem in the case of oxides with narrow nonstoichiometry field with regard to oxygen. As a rule, the exact composition with respect to oxygen is postulated in the certain ambient conditions [4] or it is computed on the basis of some model assumptions [14, 15]. Therefore, in order to determine the initial value of oxygen nonstoichiometry δ_0 in a reference state experimental data were treated as $\delta = \Delta\delta + \delta_0$, where $\Delta\ \delta$ is relative change of oxygen nonstoichiometry measured directly in the coulometric cell from a reference state, according to *models 1* and 2. The model equations Eqs. 14 and 17 were fitted to experimental data at all temperatures studied for $\mathrm{LaCoO}_{3\text{-}\delta}$. Fitting results were coincident with each other and the value of 0.001 was accepted for δ_0 in undoped lanthanum cobaltite at 1000 °C in air. This value is in good agreement with that determined using reduction method within the error range. The oxygen nonstoichiometry measured as a function of p_{O_2} and temperature for undoped $\mathrm{LaCoO}_{3\text{-}\delta}$ and adjusted as mentioned above is shown in Fig. 1.

Since the changes in oxygen stoichiometry were measured in relatively narrow temperature range for all oxide compositions studied in the present work, defect formation enthalpies can be regarded as constants over complete temperature range investigated. This assumption allows to substitute equilibrium constants in fit equations by their temperature dependences (see Eqs. 12, 15, and 26) and treat data on oxygen nonstoichiometry obtained at different temperatures simultaneously as $\delta = f$ ($p\mathrm{O}_2$, T) according to the proposed models of the defect structure.

The results of the least squares fits for $\mathrm{LaCoO}_{3\text{-}\delta}$ using *model 1* described by Eq. 14 and *model 2* described by Eq. 17 are shown in Figs. 1a and b. It is evident that there is good agreement between the experimental data and the fitting using both *model 1*and *model 2* over the complete p_{O_2} and temperature ranges investigated. The fitting results are also summarized in Table 2. As follows from this table, the correlation parameters R^2 are virtually indistinguish-

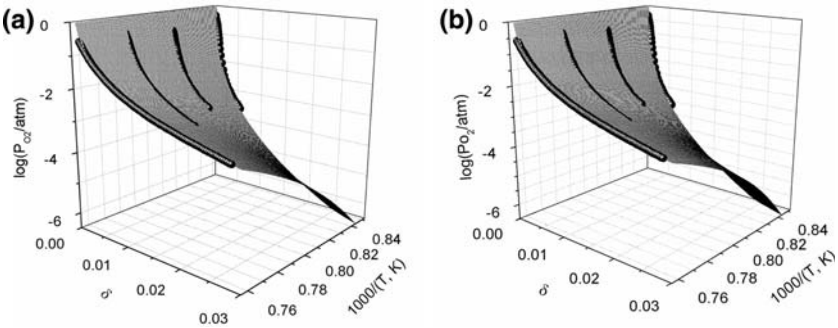

Fig. 1 Oxygen nonstoichiometry of $LaCoO_{3-\delta}$ measured as a function of p_{O_2} and temperature. Fitted surfaces are plotted on the basis of defect *model 1* (**a**) and defect *model 2* (**b**)

Table 2 The fitting results according to the defect structure models proposed

Compound	Model	Reaction, Eq.	ΔH_i (±Δ), kJ/mol	$\ln(K_0)_i$(±Δ)	*r*
$LaCoO_{3-\delta}$	1	(2)	468 (±38)	39.67 (±3.51)	0.979
		(6)	638 (± 35)	47.26 (±3.76)	
	2	(4)	691 (±46)	52.82 (±4.63)	0.979
		(10)	518 (±48)	44.96 (±4.87)	
$La_{0.7}Sr_{0.3}CoO_{3-\delta}$	1	(2)	195 (±34)	79.27 (±2.74)	0.973
		(6)	116.8 (±2.9)	119.23 (±28.52)	
	2	(4)	140 (±14)	231.4 (±11.9)	0.987
		(10)	397 (±28)	78.2 (±23.6)	
$LaCo_{0.7}Cu_{0.3}O_{3-\delta}$	1A	(2)	161.38 (–)	53.83 (–)	0.989
		(20)	107.95 (–)	43.52 (–)	
		(24)	112.28 (–)	51.86 (–)	
	2A	(4)	175.96 (–)	68.3 (–)	0.99
		(22)	100.32 (–)	33.4 (–)	
		(24)	101.82 (–)	41.76 (–)	

able for the two suggested models. The oxygen nonstoichiometry of Sr-doped $La_{0.7}Sr_{0.3}CoO_{3-\delta}$ measured as $\delta = f(p_{O_2}, T)$ and surfaces fitted according to the model expressions Eqs. 14 and 17 are shown in Figs. 2a and b, respectively. The appropriate fitting results are given in Table 2. These results obviously indicate that both models of the defect structure suggested for Sr-doped lanthanum cobaltites fit the experimental data about equally good like it was for undoped $LaCoO_{3-\delta}$. The data on oxygen nonstoichiometry of $LaCo_{0.7}Cu_{0.3}O_{3-\delta}$ and surfaces fitted on the basis of the models 1A and 2A are shown in Figs. 3a and b, respectively. Comparison of these figures reveals that the question of whether holes are localized on cobalt sites in the Cu-doped lanthanum cobaltite or not remains open as well. The latter is also confirmed by about equal correlation parameters for both models given in Table 2.

The equilibrium constants of defects reactions obtained in this work by nonlinear curve fitting allow to calculate the isothermal dependencies of point defect concentration on oxygen nonstoichiometry or oxygen partial pressure. Such dependences, for instance, are shown in Figs. 4–6 for $LaCoO_{3-\delta}$, $La_{0.7}Sr_{0.3}CoO_{3-\delta}$, and $LaCo_{0.7}Cu_{0.3}O_{3-\delta}$, respectively, at selected temperatures. As can be seen in these figures, the

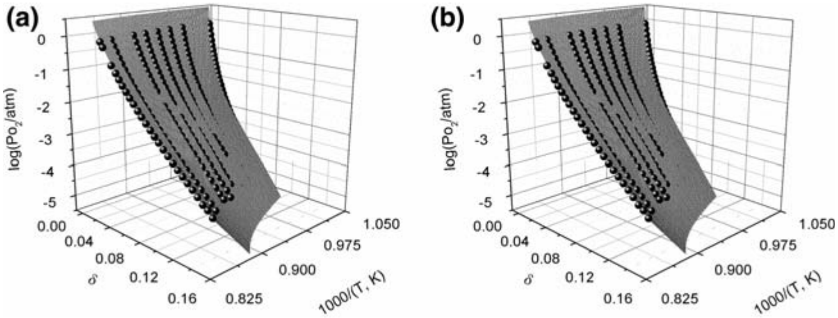

Fig. 2 Oxygen nonstoichiometry of $La_{0.7}Sr_{0.3}CoO_{3-\delta}$ measured as a function of p_{O_2} and temperature [11]. Fitted surfaces are plotted on the basis of defect *model 1* (**a**) and defect *model 2* (**b**)

Fig. 3 Oxygen nonstoichiometry of $LaCo_{0.7}Cu_{0.3}O_{3-\delta}$ measured as a function of p_{O_2} and temperature. Fitted surfaces are plotted on the basis of defect *model 1A* (**a**) and defect *model 2A* (**b**)

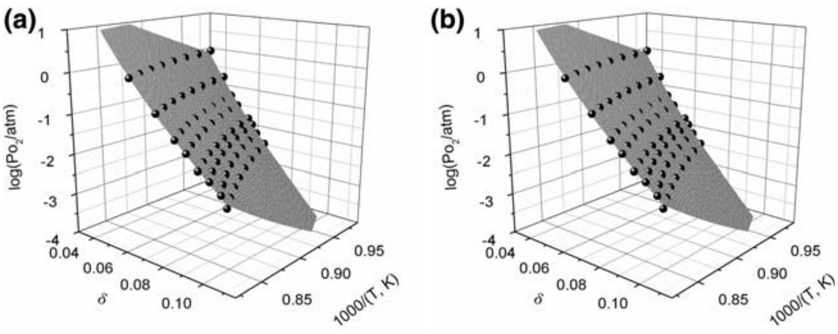

Fig. 4 Changes of concentration of different defect species in $LaCoO_{3-\delta}$ computed on the basis of defect *model 1* (**a**) and defect *model 2* (**b**) at 1050 °C

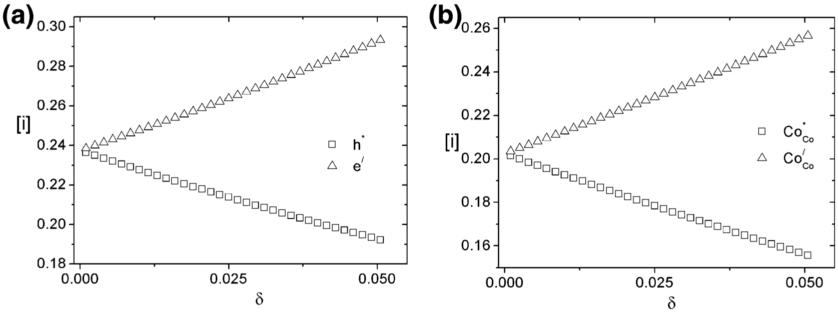

Fig. 5 Changes of concentration of different defect species in $La_{0.7}Sr_{0.3}CoO_{3-\delta}$ computed on the basis of defect *model 1* (**a**) and defect *model 2* (**b**) at 900 °C

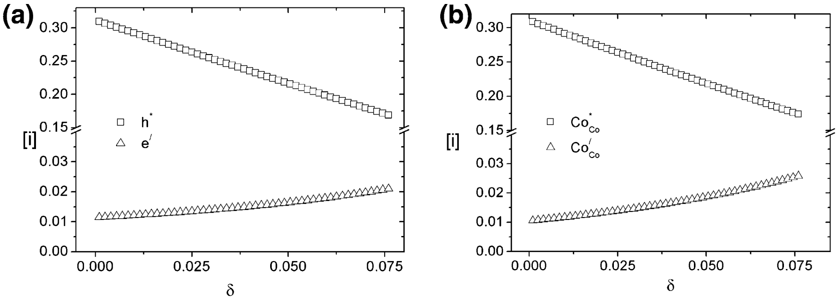

Fig. 6 Changes of concentration of different defect species in $LaCo_{0.7}Cu_{0.3}O_{3-\delta}$ computed on the basis of defect *model 1A* (**a**) and defect *model 2A* (**b**) at 950 °C

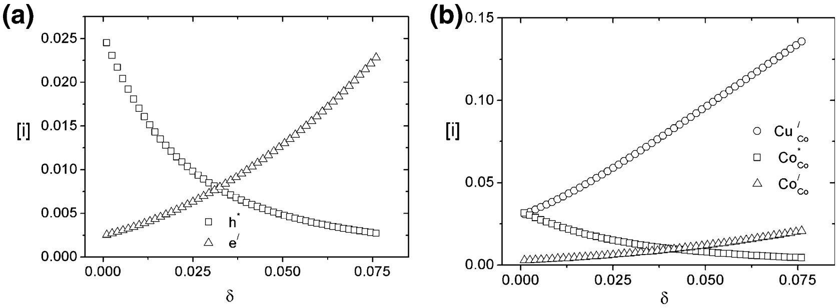

trends in changes of concentration of electrons and holes with oxygen nonstoichiometry are similar irrespective of the nature of electronic defects. The second particularity following from these figures is that the holes concentration in copper doped cobaltite $LaCo_{0.7}Cu_{0.3}O_{3-\delta}$ is less than that in strontium doped $La_{0.7}Sr_{0.3}CoO_{3-\delta}$ by about a factor of order of magnitude under the same conditions. This obviously indicates that formation of negative charged defects Cu'_{Co} is accompanied rather by oxygen vacancies formation according to reaction Eq. 24 than that of holes. It is of interest to note that similar trend was recently reported for copper doped lanthanum chromite $LaCr_{0.79}Cu_{0.05}Al_{0.16}O_{3-\delta}$ with the same crystal structure [16]. Addition of copper in chromite was found to result in oxygen vacancies formation and does not change the chromium oxidation state of 3+ over the complete oxygen partial pressure range investigated. In contrast to this, copper was shown to change its oxidation state continuously from 3+ via 2+ to 1+ if the oxygen partial pressure decreases.

Conclusions

The modeling of the defect structure of the oxygen deficient lanthanum cobaltites undoped and doped with acceptor dopants Sr and Cu on A and B site, respectively, was evolved. Noteworthy features of this modeling are the following: (i) The models on the basis of itinerant and localized electronic defects were considered for both undoped and doped lanthanum cobaltites. (ii) Thermal excited charge disproportionation of cobalt and intrinsic electronic disordering process (creation/annihilation of quasi-free holes and electrons) were taken into account as well. (iii) The analytical solution of a set of independent equations yielded a general expression which allowed to establish agreement between the measured properties (oxygen nonstoichiometry and oxygen partial pressure) and the proposed models by nonlinear curve fitting. (iv) Equilibrium constants were determined which yielded the equilibrium concentration of all defect species for a given oxygen partial pressure and temperature.

Two particularities have to be highlighted: (1) The models of the defect structure based on the itinerant and localized nature of electronic defects fit the experimental data on oxygen nonstoichiometry of undoped and doped with Sr and Cu lanthanum cobaltites about equally good. It is, therefore, difficult to rule out either of defect structure models on the basis of equilibrium data on oxygen nonstoichiometry solely. (2) Addition of copper in $LaCoO_{3-\delta}$ seems to lead to appearance of the negative charged defects Cu'_{Co} and oxygen vacancies formation according to reaction Eq. 24 rather than that of holes unlike the case of doping with strontium.

Acknowledgements This work was supported by the Russian Foundation for Basic Research (grants Nos. 04-03-32142 and 06-08-08120) and the US Civilian Research & Development Foundation (project REC-005).

References

1. Jonker GH (1969) Philips Res Rep 24:1
2. Zuev AYu, Petrov AN, Pankov DV (1999) In: Singhal SC, Dokia M (eds) Solid oxide fuel cells VI, The Electrochemical Society Proceedings Series, PV 99–19, 424, Pennington, NJ
3. Yasumoto K, Inagaki Y, Shiono M, Dokiya M (2002) Solid State Ionics 148:545
4. Mizusaki J, Mima Y, Yamauchi S, Fueki K, Tagawa H (1989) J Solid State Chem 80:102
5. Petrov AN, Cherepanov VA, Kononchuk OF, Gavrilova LYa (1990) J Solid State Chem 87:69
6. Petrov AN, Kononchuk OF, Andreev AV, Cherepanov VA, Kofstad P (1995) Solid State Ionic 80:189
7. Lankhorst MHR, Bouwmeester HJM, Verweij H (1996) Physical Rev Lett 77:2989
8. Lankhorst MHR, Bouwmeester HJM, Verweij H (1997) J Solid State Chem 133:555
9. Lankhorst MHR, Bouwmeester HJM, Verweij H (1997) Solid State Ionics 96:21
10. Patrakeev MV, Leonidov IA, Mitberg EB, Lakhtin AA, Vasiliev VG, Kozhevnicov VL, Poeppelmeier KR (1999) Ionics 5:444
11. Kozhevnikov VL, Leonidov IA, Mitberg EB, Patrakeev MV, Petrov AN, Poeppelmeier KR (2003) J Solid State Chem 172:296
12. Petrov AN, Zuev AYu, Pankov DV, Bujanova EC (2004) Russian J Phys Chem 78:220
13. Petrov AN, Zuev AYu, Pankov DV (2004) Russian J Phys Chem 78:1616
14. Seppaenen M, Kytoe M, Taskinen P (1980) Scand J Met 9:3
15. Petrov AN, Cherepanov VA, Zuev AYu (1987) Russian J Phys Chem 61:630
16. Zuev A, Singheiser L, Hilpert K (2005) Solid State Ionics 176:417